Insights from Earth body tide data on mantle anelasticity

Lambert Caron[1], Erik Roman Ivins[1], Surendra Adhikari[1], Holly Kyeore Han[1] and Luc Houriez[2]
(1)Jet Propulsion Laboratory, Pasadena, United States
(2)Stanford University, Stanford, United States

Government sponsorship acknowledged.

Deformation at the microscopic level

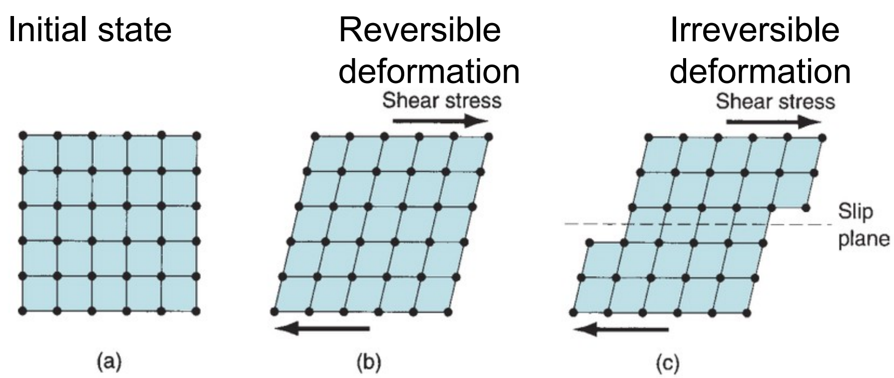

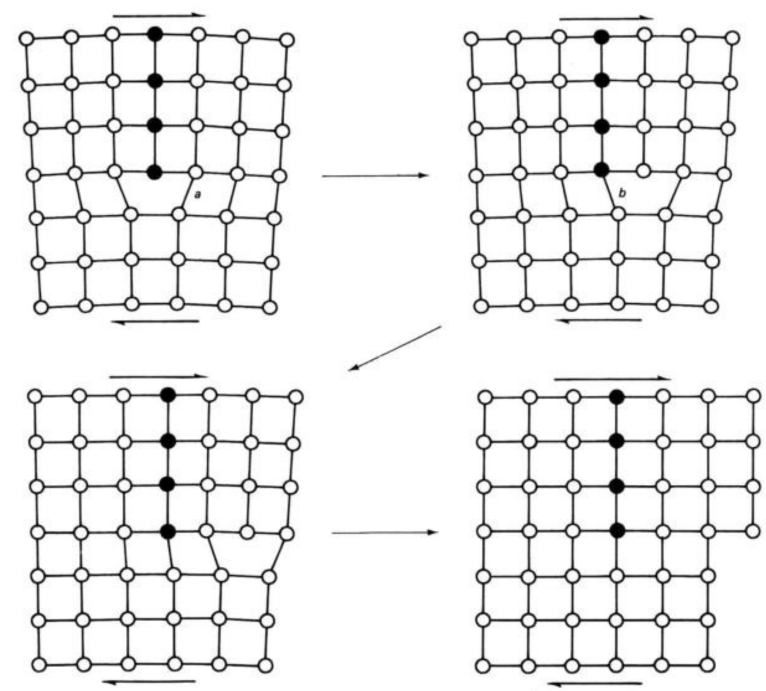

(Translation of a stressed edge dislocation)

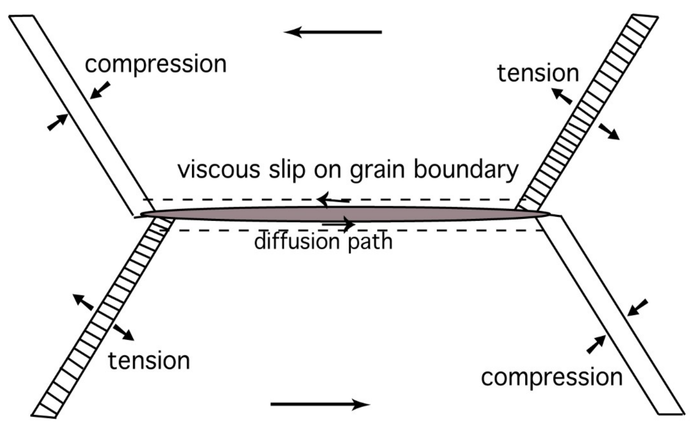

Diffusion accomodated grain boundary sliding (viscous)

- Elastic (reversible) vs viscous (irreversible) deformation
- Different mechanisms or regimes within and between grains
- Dependence on pressure, temperature, composition, grain size, water content, etc
- Modeling requires compromise between fidelity and complexity that can be data constrained

Evidence for anelasticity

- Traditional understanding: viscosity is important at 100yr and longer time scales (GIA). Elasticitv is sufficient below

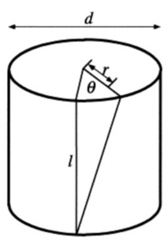

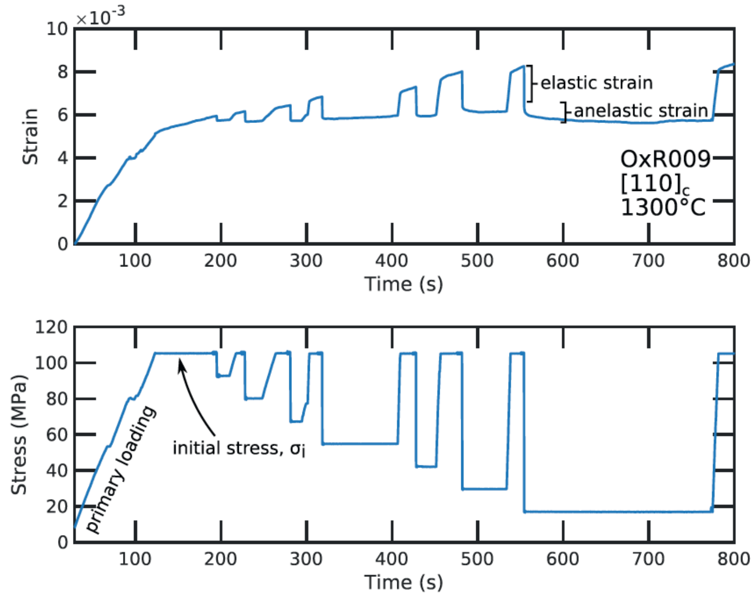

Laboratory experiment shows transient relaxation in single crystal deformation (Hansen et al 2021)

Dunite torsion experiments (J and Faul 2014)

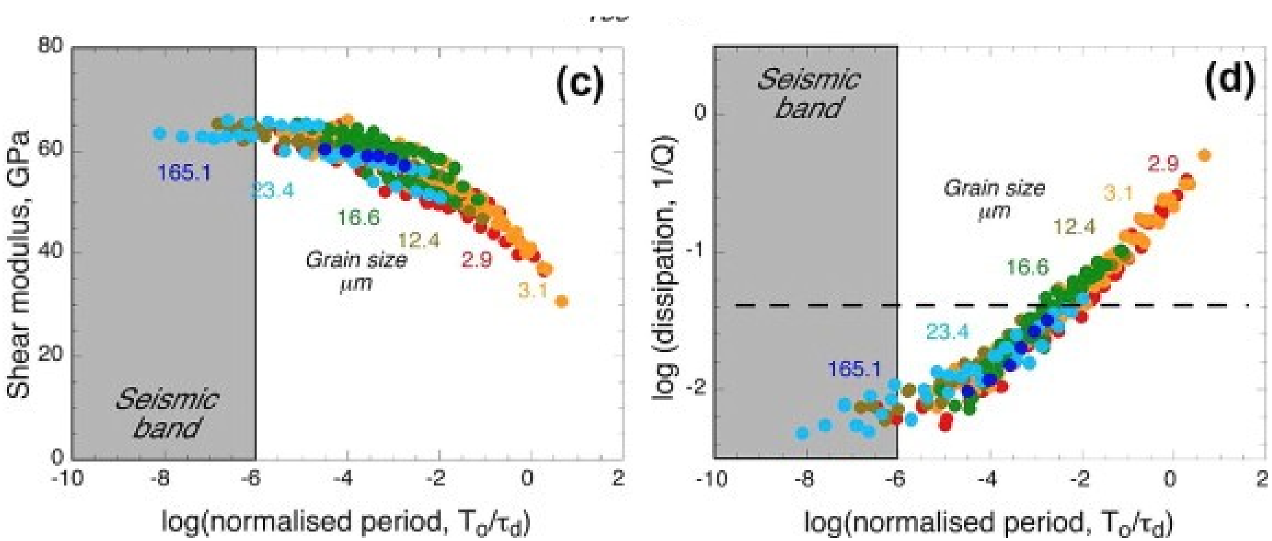

Transient viscosity model based on mineral physics constraints (Breithaupt et al 2023)

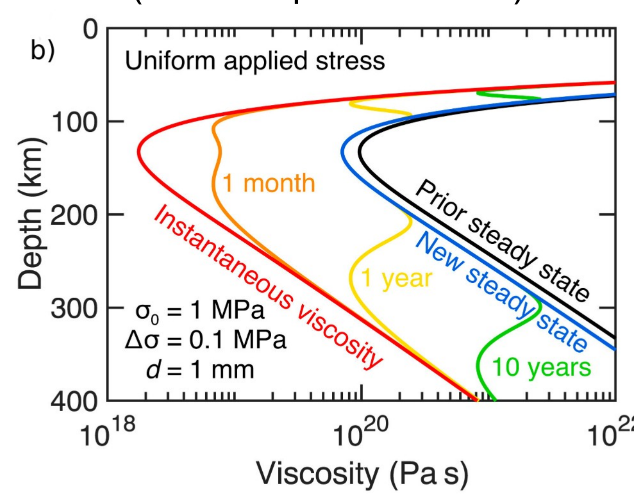

Evidence for anelasticity

- Traditional understanding: viscosity is important at 100yr and longer time scales (GIA). Elasticity is sufficient below

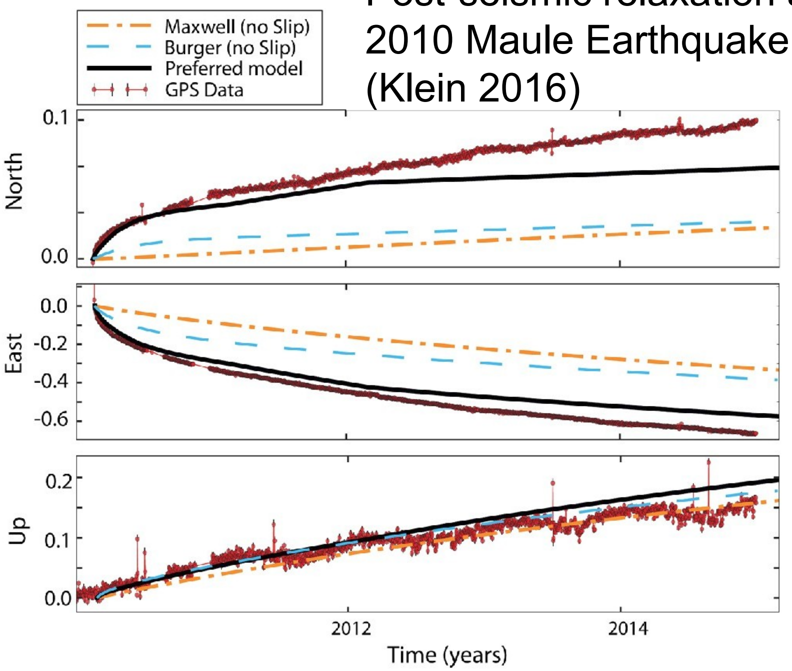

Post-seismic relaxation after the 2010 Maule Earthquake, Chile (Klein 2016)

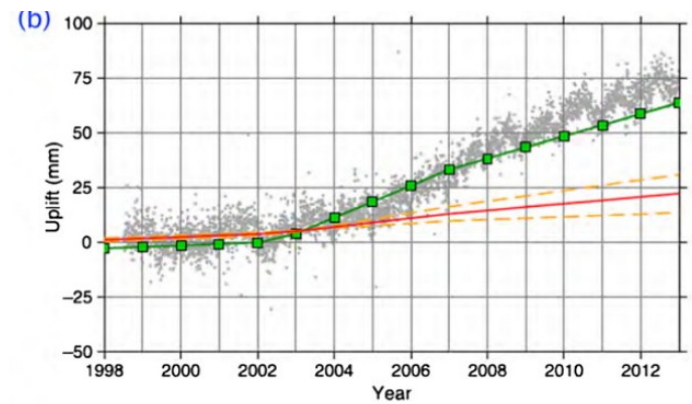

Red: Elastic
Orange: Elastic + uncertainty
Green: Low viscosity Maxwell

GPS uplift after the collapse of the Larsen B ice shelf, Antarctic Peninsula (Nield et al 2014)
See also Hazzard et al (2021)

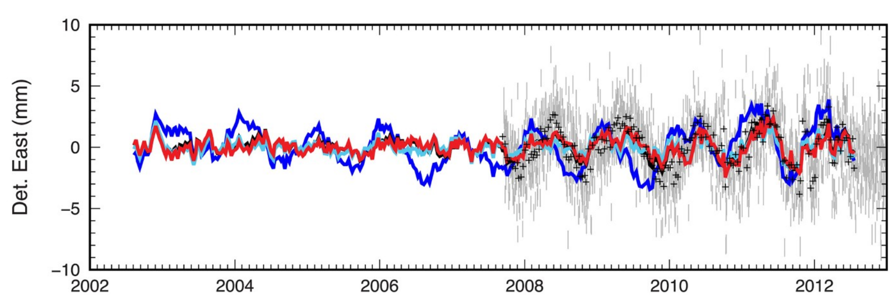

a. Seasonal water loading response: model fitness improved by viscous asthenosphere (Chanard et al 2018)

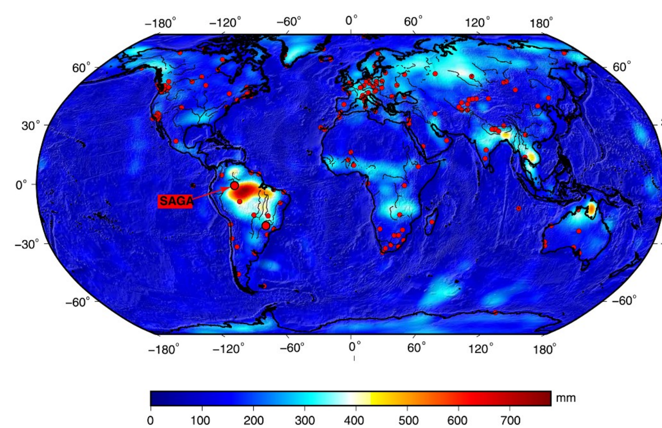

b. Seasonal water cycle strength and GPS network

Anelasticity in body tides

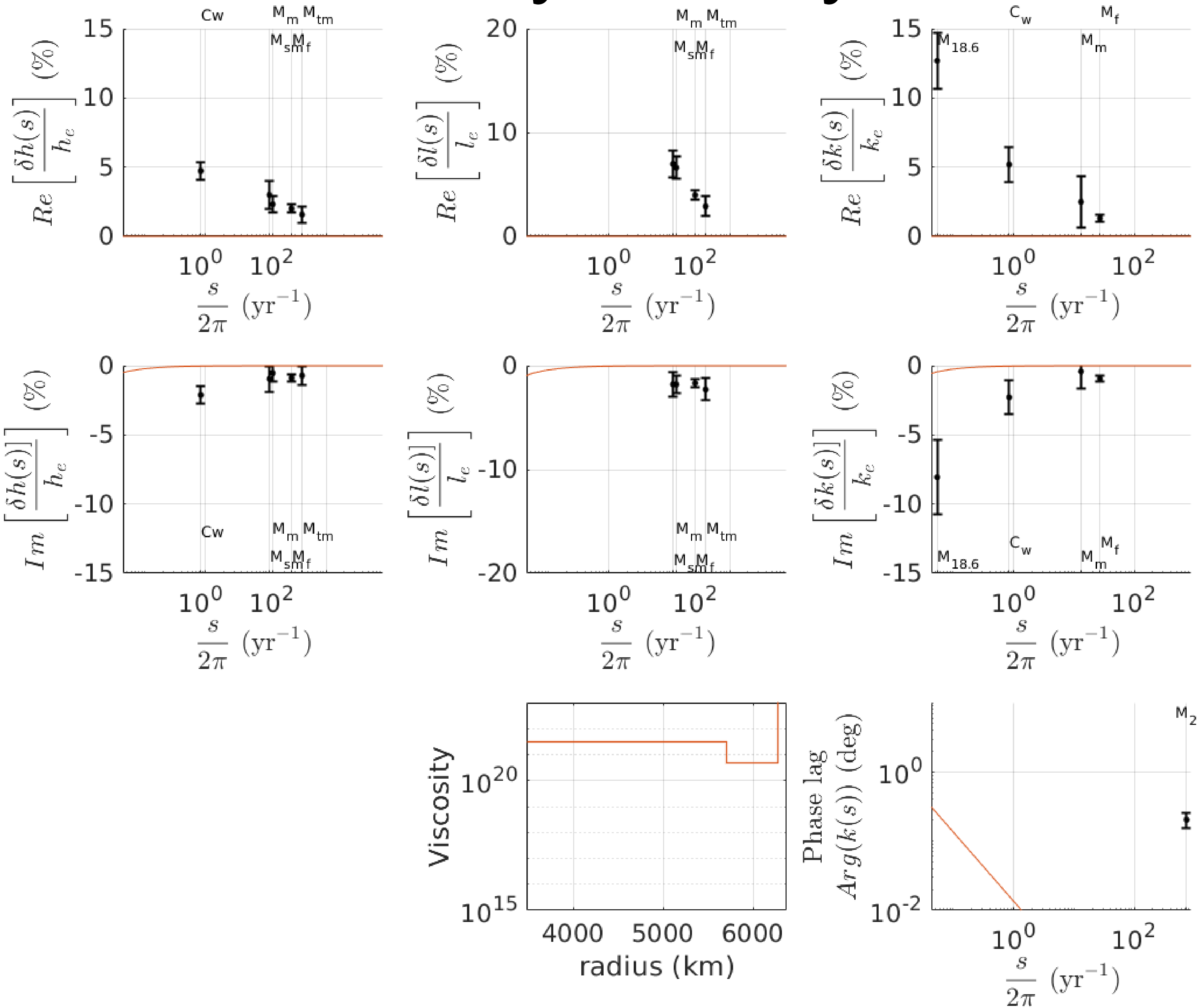

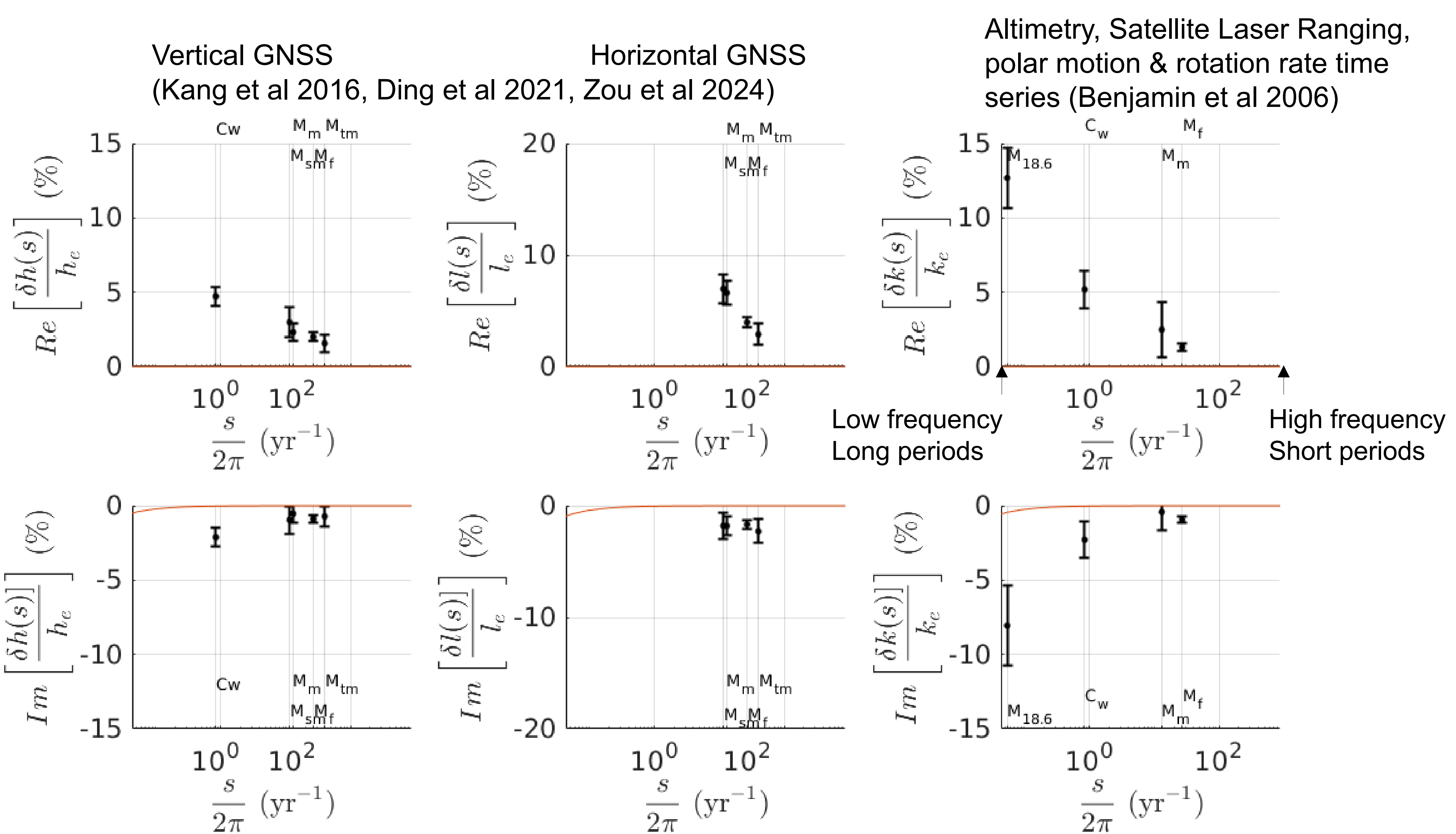

Measures the % difference of the solid-Earth tidal response compared to a purely elastic behavior

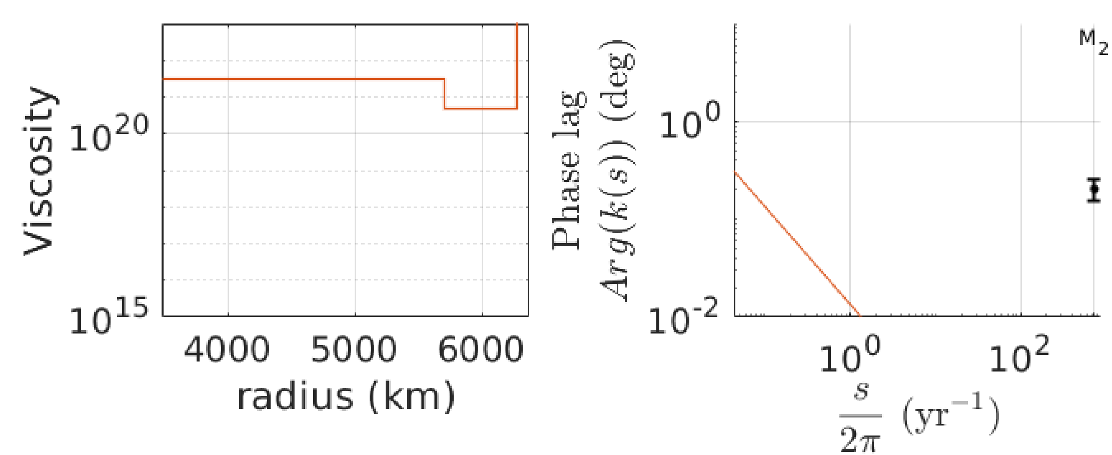

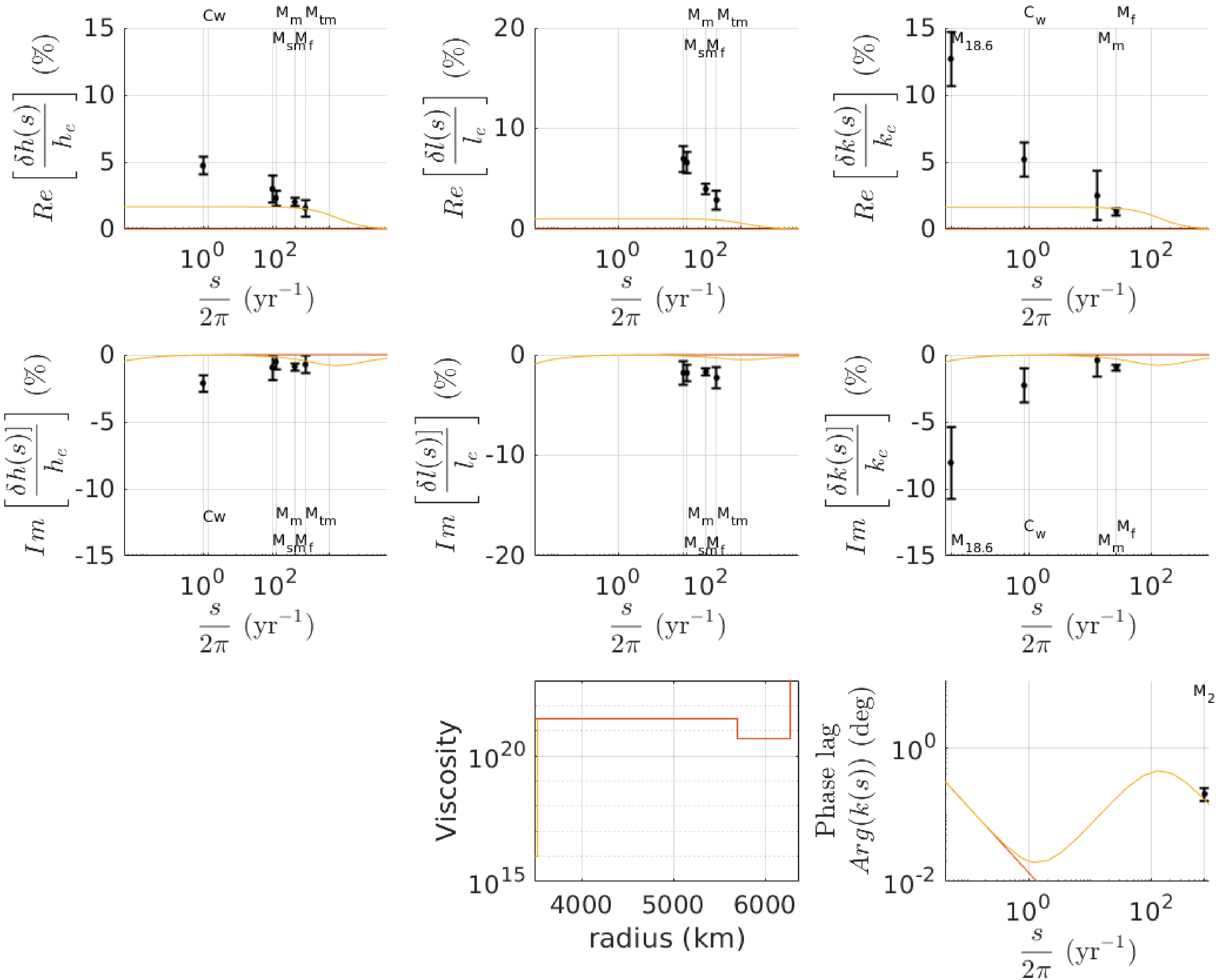

Cw
M_m M_{tm}
M_{sm} M_f
$Re\left[\frac{\delta h(s)}{h_e}\right]$ (%)
$Re\left[\frac{\delta l(s)}{l_e}\right]$ (%)
$M_{18.6}$
C_w
$Re\left[\frac{\delta k(s)}{k_e}\right]$ (%)
$\frac{s}{2\pi}$ (yr^{-1})
$Im\left[\frac{\delta h(s)}{h_e}\right]$ (%)
$Im\left[\frac{\delta l(s)}{l_e}\right]$ (%)
$Im\left[\frac{\delta k(s)}{k_e}\right]$ (%)
Viscosity
radius (km)
Phase lag
$Arg(k(s))$ (deg)
M_2

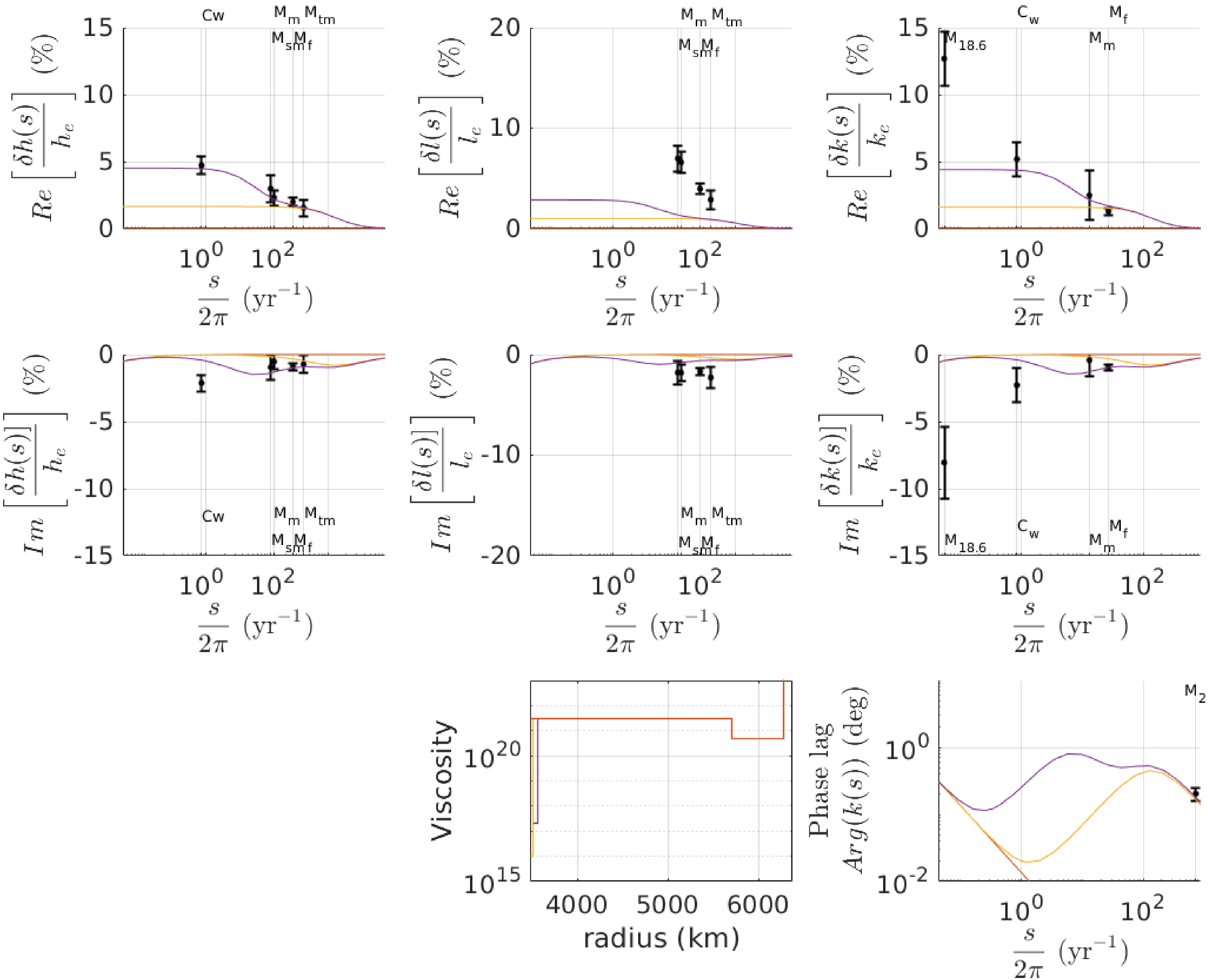

Cw
Mm Mtm
Msm Mf
Re [δh(s)/he] (%)
Re [δl(s)/le] (%)
C_w
M_f
M_18.6
M_m
Re [δk(s)/ke] (%)
s/2π (yr⁻¹)
Im [δh(s)/he] (%)
Im [δl(s)/le] (%)
Im [δk(s)/ke] (%)
Viscosity
radius (km)
Phase lag
Arg(k(s)) (deg)
M_2

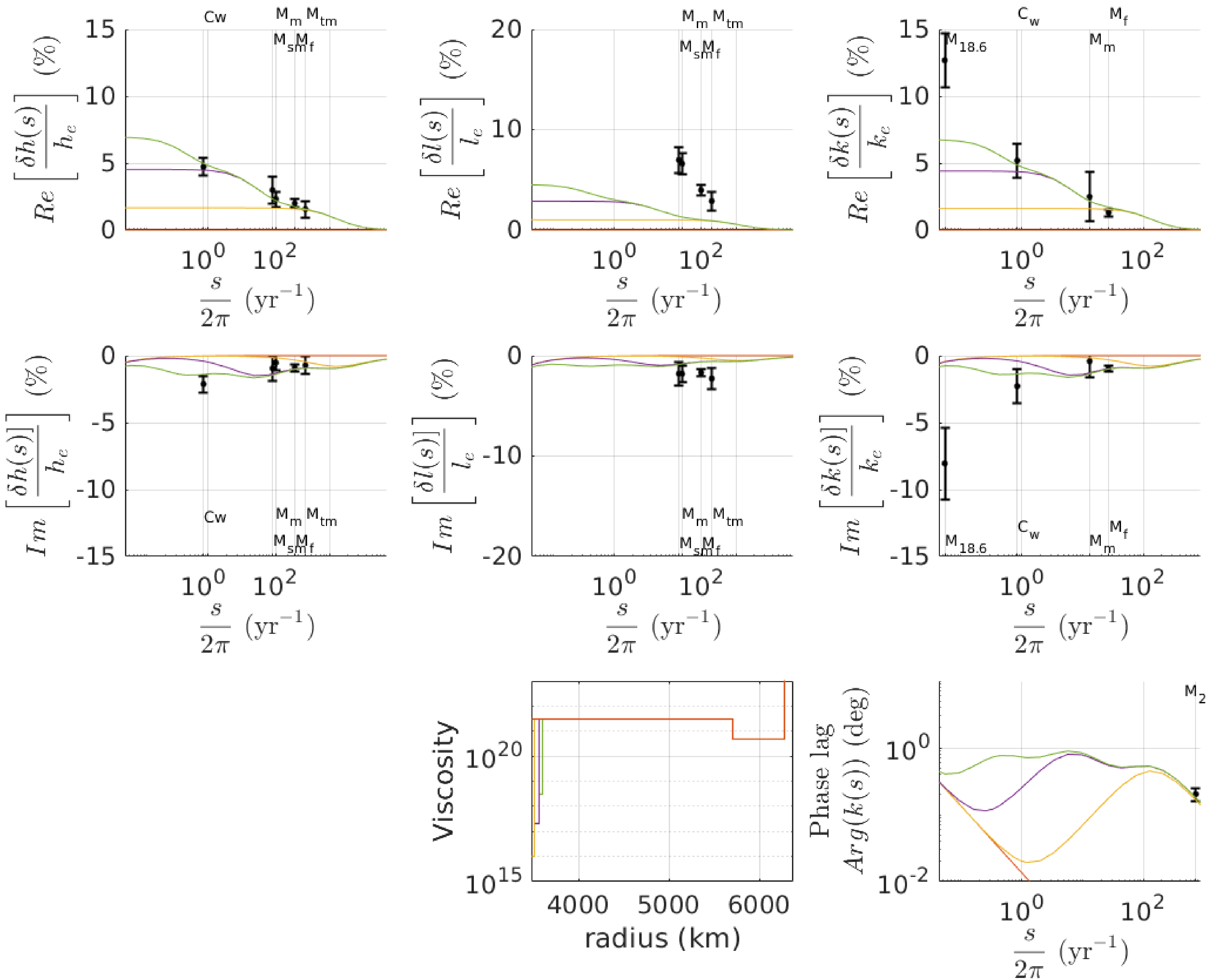
Cw
M_m M_tm
M_sm M_f
Re [δh(s)/h_e] (%)
Re [δl(s)/l_e] (%)
C_w
M_f
M_18.6
M_m
Re [δk(s)/k_e] (%)
s/2π (yr^-1)
Im [δh(s)/h_e] (%)
Im [δl(s)/l_e] (%)
Im [δk(s)/k_e] (%)
Viscosity
radius (km)
Phase lag
Arg(k(s)) (deg)
M_2

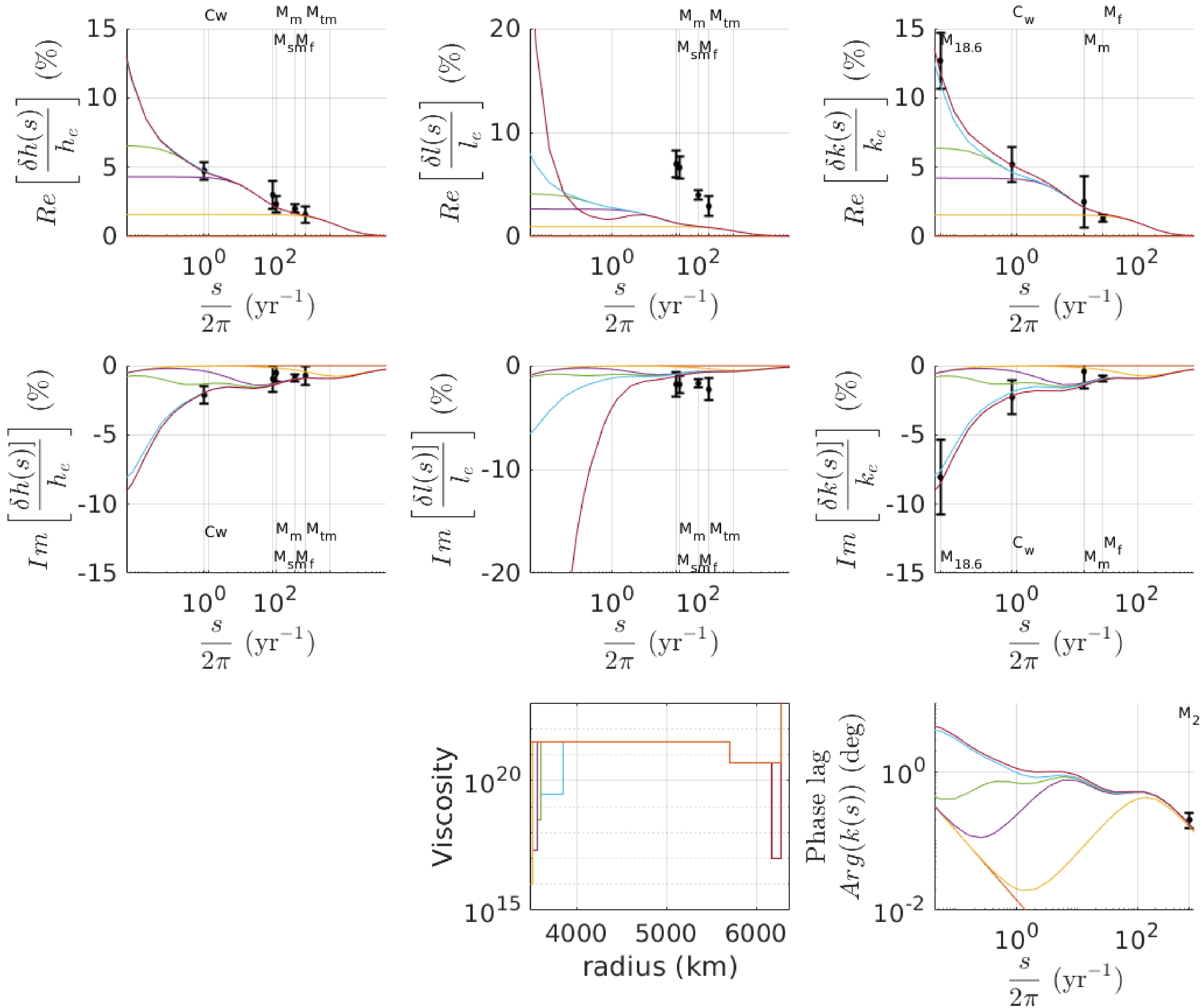

Cw
M_m M_{tm}
M_{sm} M_f
C_w
$M_{18.6}$
$Re\left[\frac{\delta h(s)}{h_e}\right]$ (%)
$Re\left[\frac{\delta l(s)}{l_e}\right]$ (%)
$Re\left[\frac{\delta k(s)}{k_e}\right]$ (%)
$Im\left[\frac{\delta h(s)}{h_e}\right]$ (%)
$Im\left[\frac{\delta l(s)}{l_e}\right]$ (%)
$Im\left[\frac{\delta k(s)}{k_e}\right]$ (%)
$\frac{s}{2\pi}$ (yr^{-1})
Viscosity
radius (km)
Phase lag
$Arg(k(s))$ (deg)
M_2

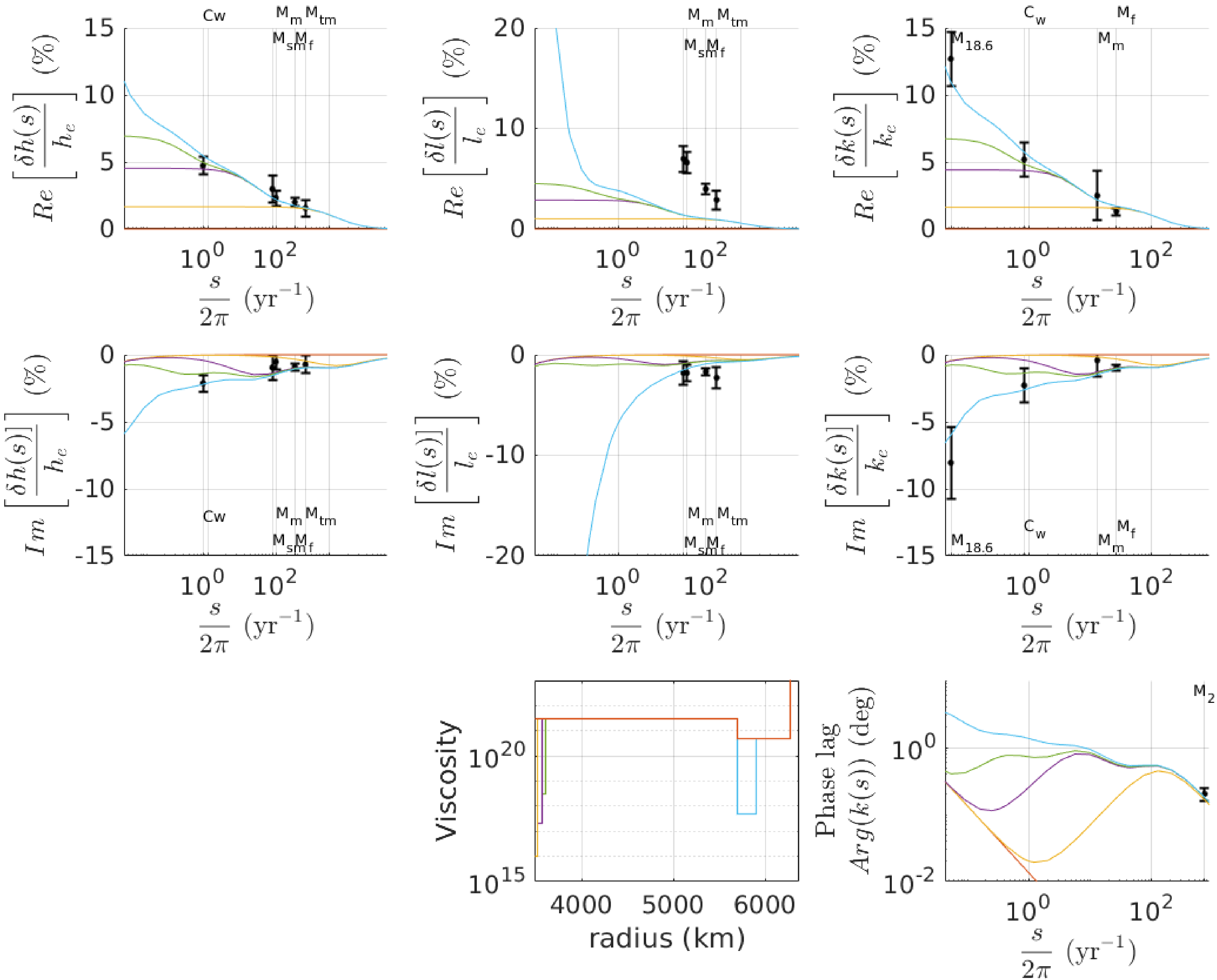

Cw
Mm Mtm
Msm Mf
15
10
5
0
Re [δh(s)/he] (%)
10^0
10^2
s/2π (yr^-1)
Mm Mtm
Msm Mf
20
10
0
Re [δl(s)/le] (%)
Cw
Mf
Mm
M18.6
Re [δk(s)/ke] (%)
-5
-10
-15
Im [δh(s)/he] (%)
-20
Im [δl(s)/le] (%)
Im [δk(s)/ke] (%)
Viscosity
10^20
10^15
4000
5000
6000
radius (km)
M2
Phase lag
Arg(k(s)) (deg)
10^0
10^-2

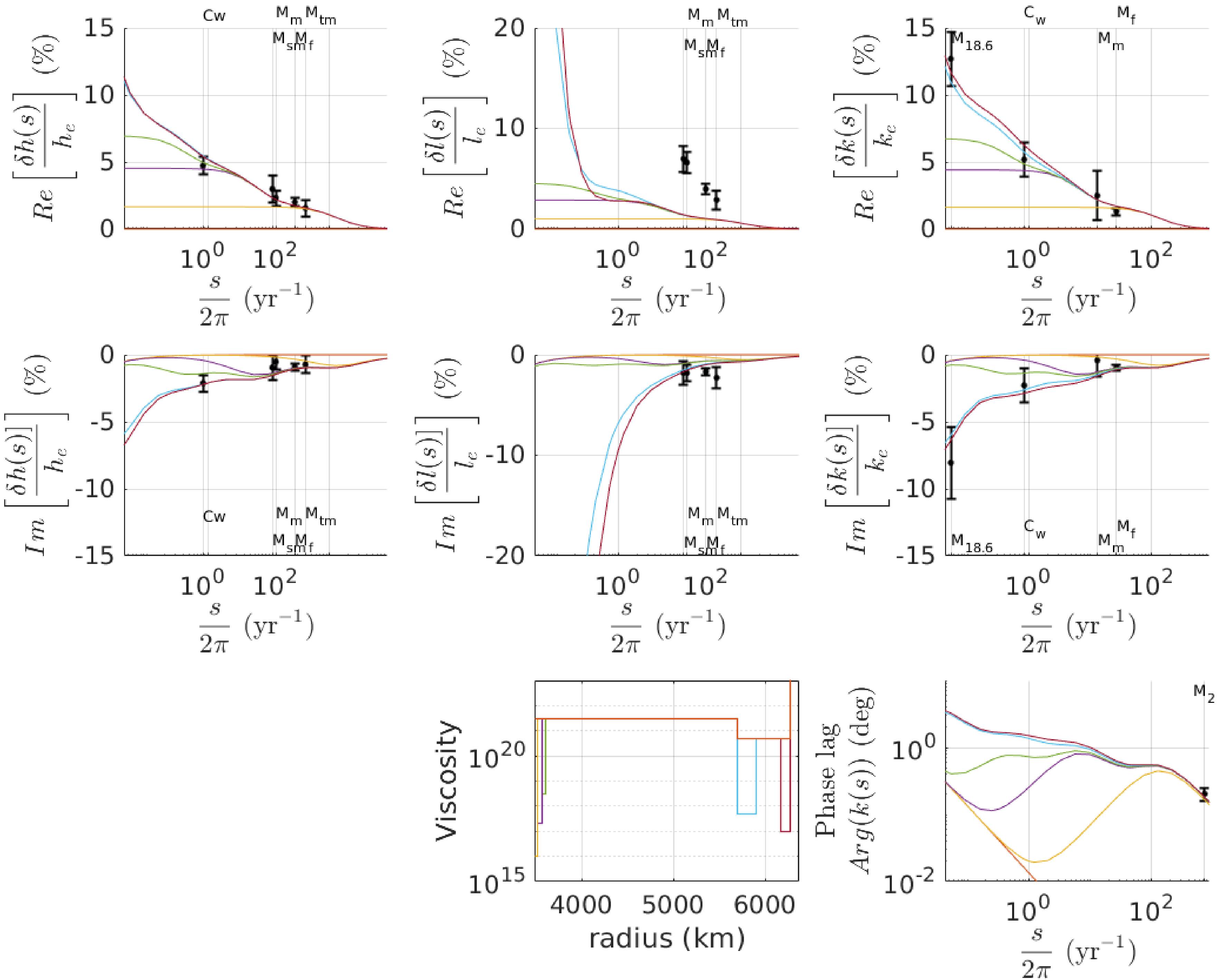

Cw
M_m M_{tm}
M_{sm} M_f
$Re\left[\frac{\delta h(s)}{h_e}\right]$ (%)
$Re\left[\frac{\delta l(s)}{l_e}\right]$ (%)
$Re\left[\frac{\delta k(s)}{k_e}\right]$ (%)
$M_{18.6}$
C_w
$Im\left[\frac{\delta h(s)}{h_e}\right]$ (%)
$Im\left[\frac{\delta l(s)}{l_e}\right]$ (%)
$Im\left[\frac{\delta k(s)}{k_e}\right]$ (%)
$\frac{s}{2\pi}$ (yr^{-1})
Viscosity
radius (km)
Phase lag
$Arg(k(s))$ (deg)
M_2

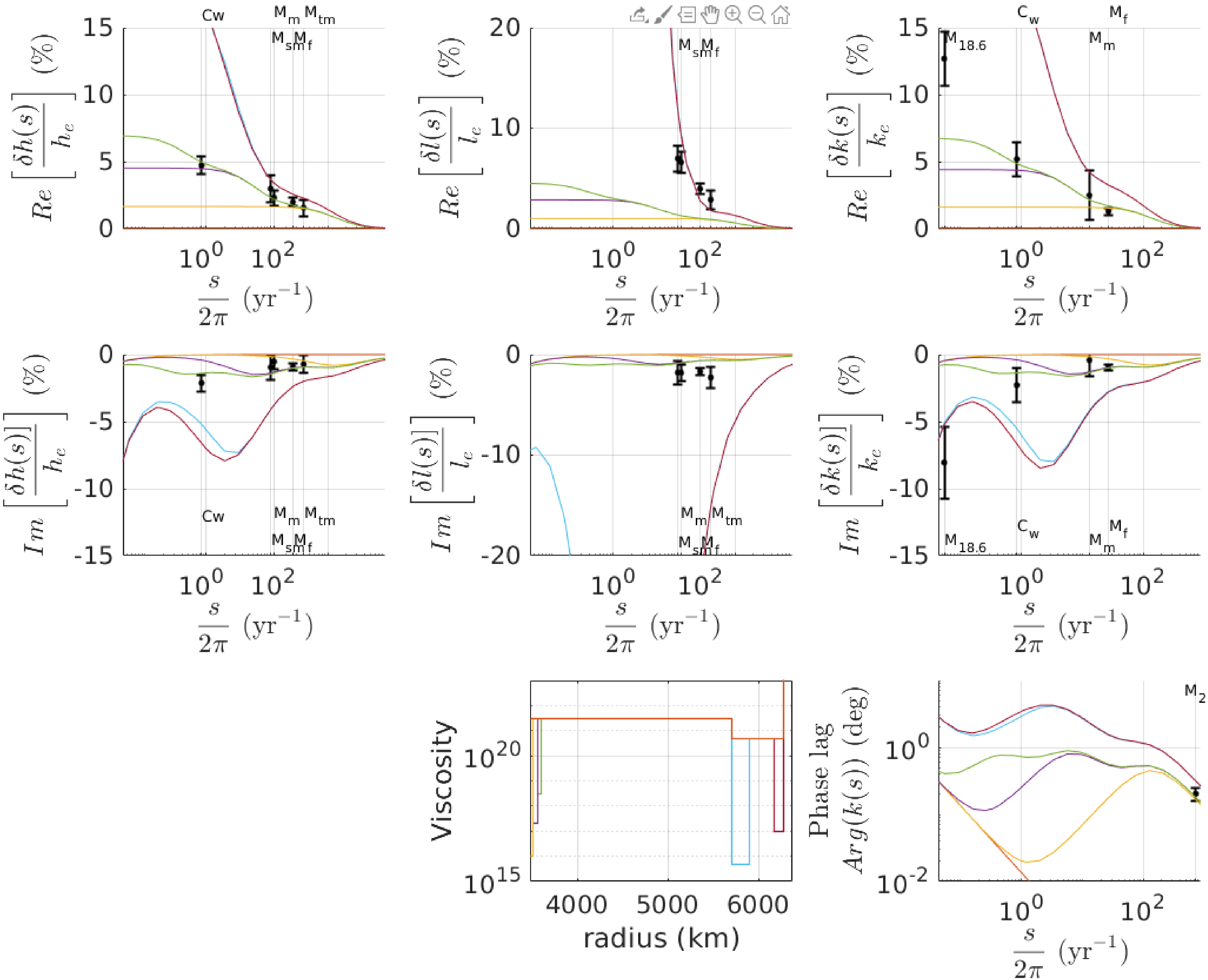
Cw
Mm Mtm
Msm Mf
Re [δh(s)/he] (%)
s/2π (yr^-1)
Re [δl(s)/le] (%)
Re [δk(s)/ke] (%)
M18.6
Cw
Mf
Mm
Im [δh(s)/he] (%)
Im [δl(s)/le] (%)
Im [δk(s)/ke] (%)
Viscosity
radius (km)
Phase lag
Arg(k(s)) (deg)
M2

Steady-state viscosity in the D” layer and Transition zone

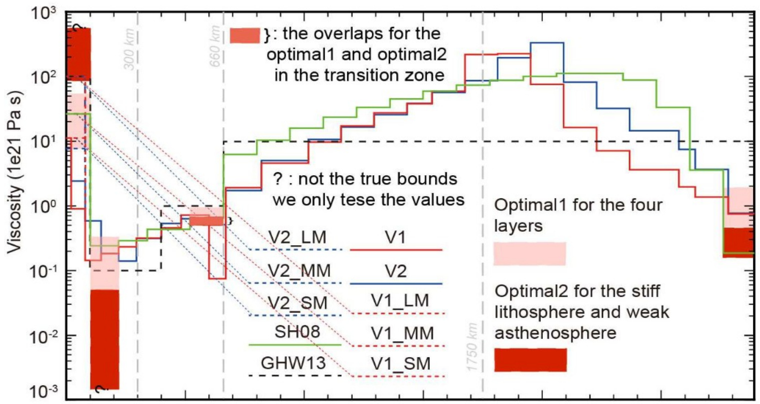

Wang et al (2020)

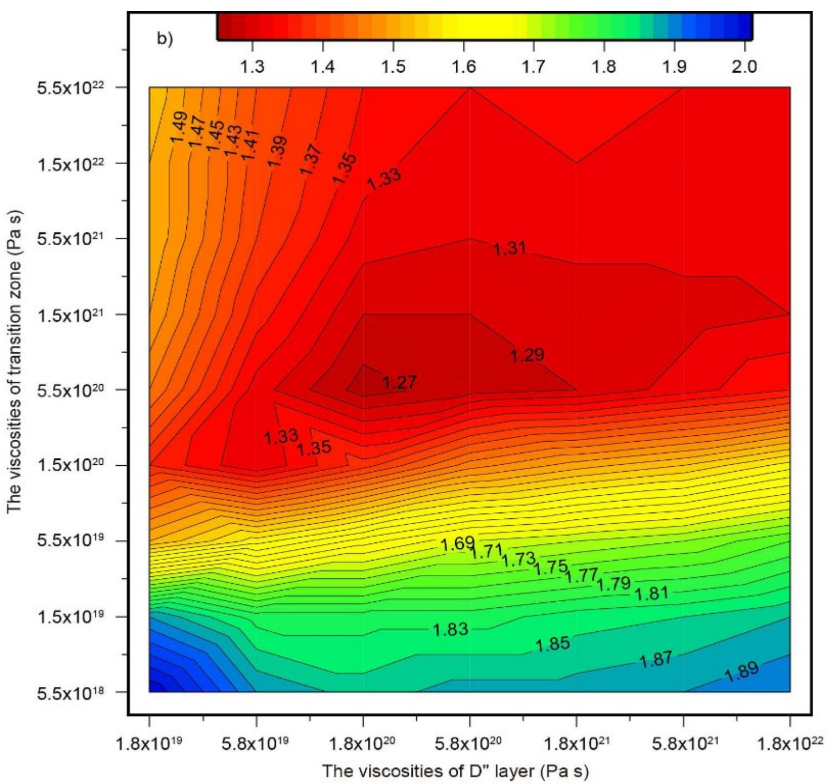

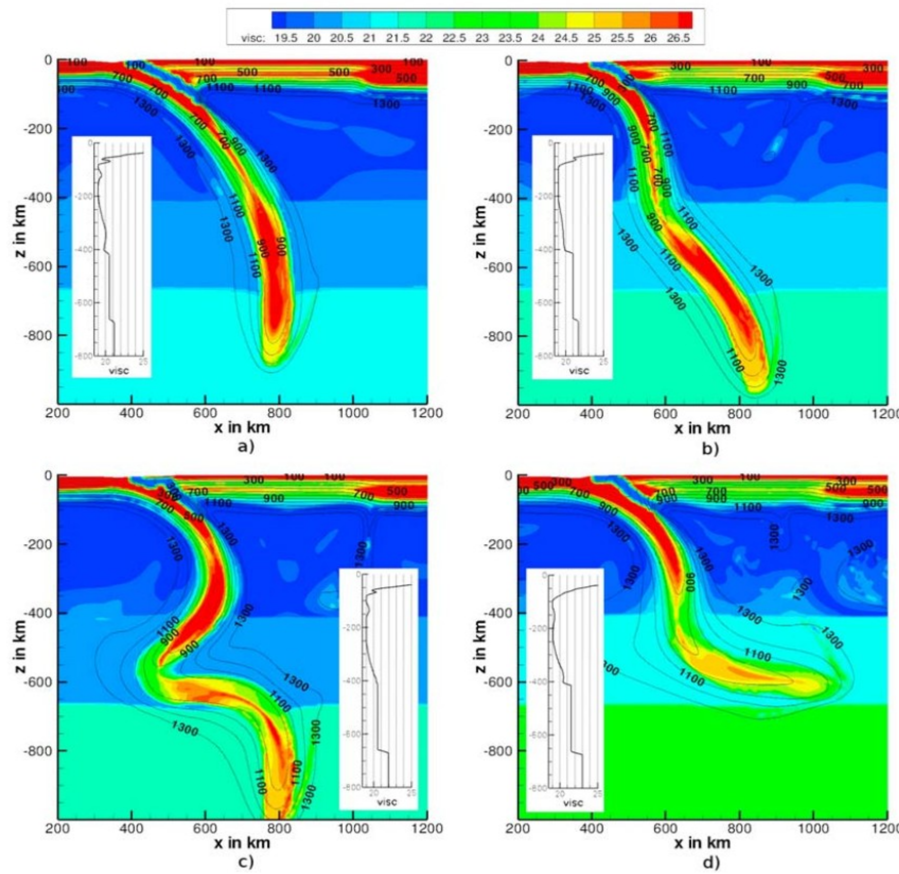

Quinteros et al (2010)

TZ: 3–10 * 10^20 Pa s (slab velocities at the 660km discontinutiy)

5–9 * 10^20 Pa s (geoid anomalies)

D” : 1.6–18 * 10^20 Pa s (geoid anomalies)

The Extended Burgers Material

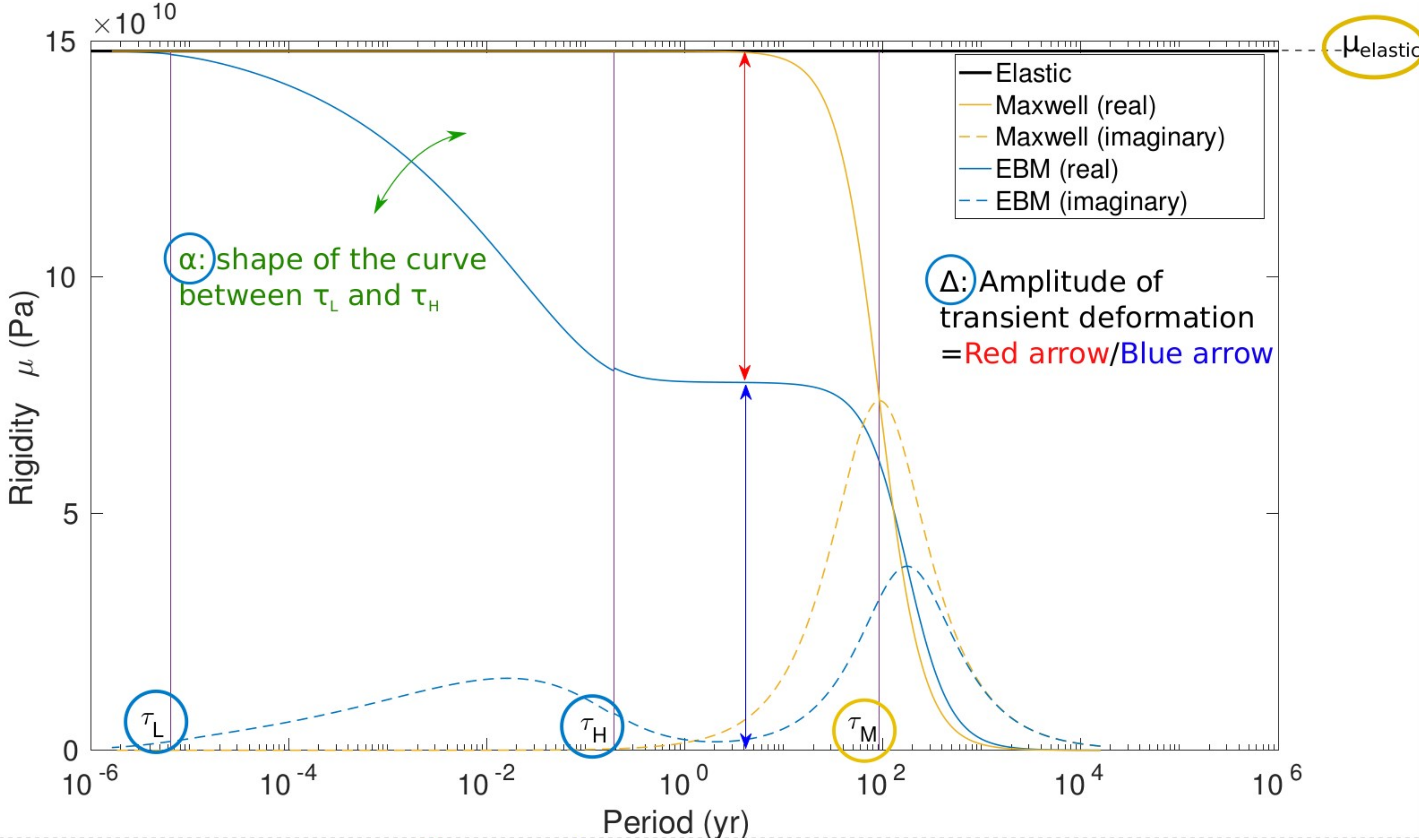

EBM Parameter exploration

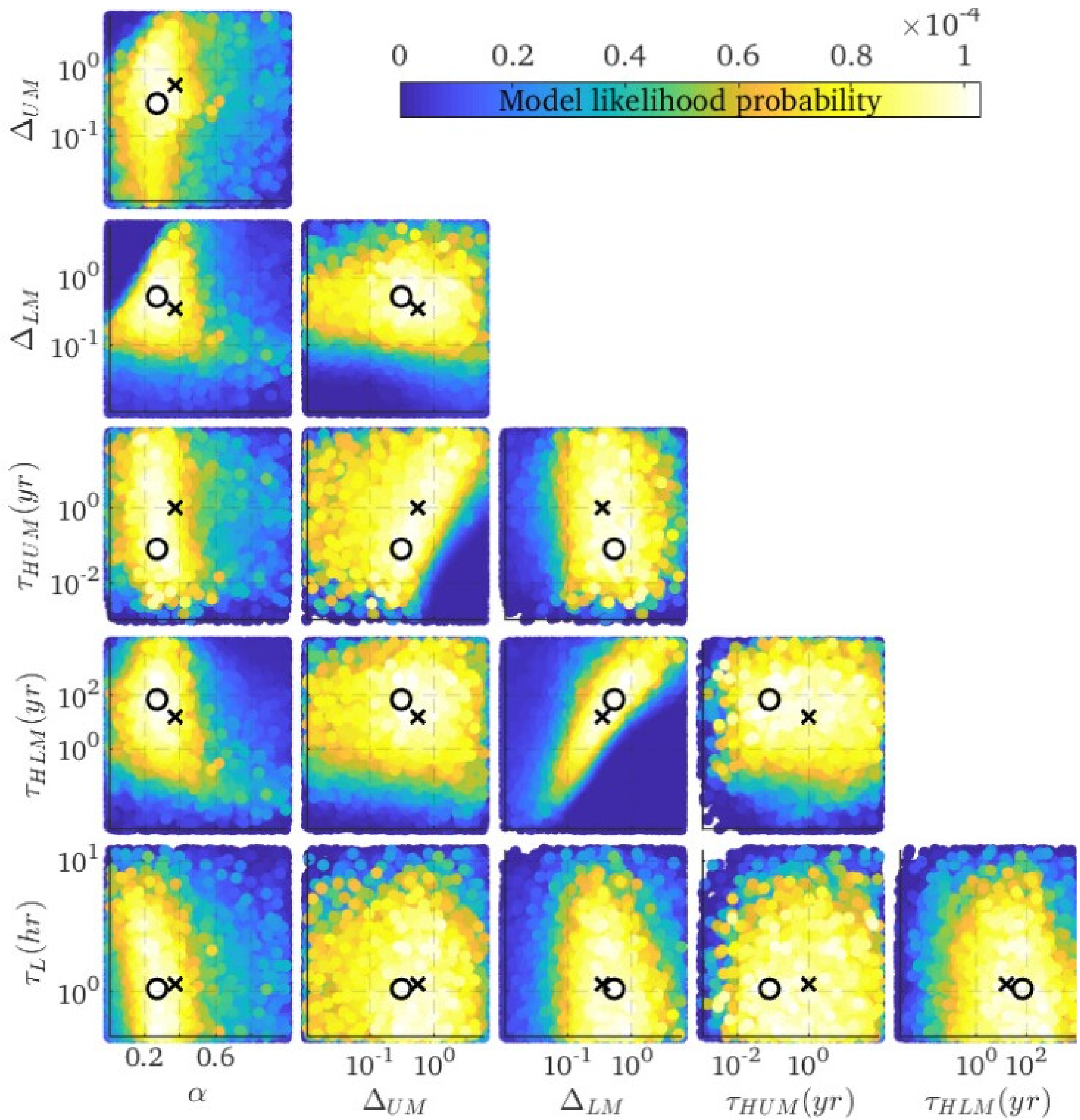

Anelasticity in body tides with EBM

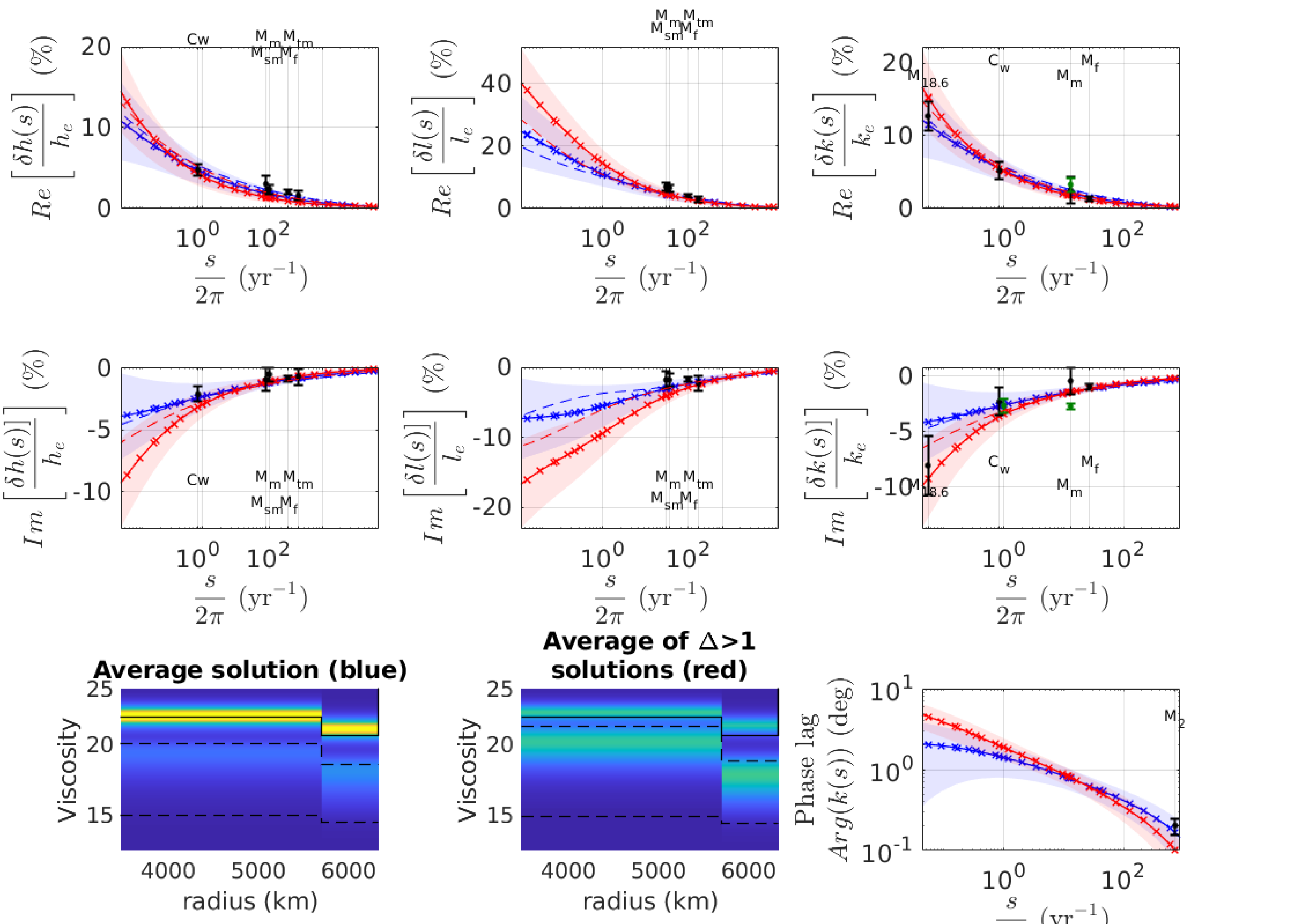

Reconciling geodynamics and GIA?

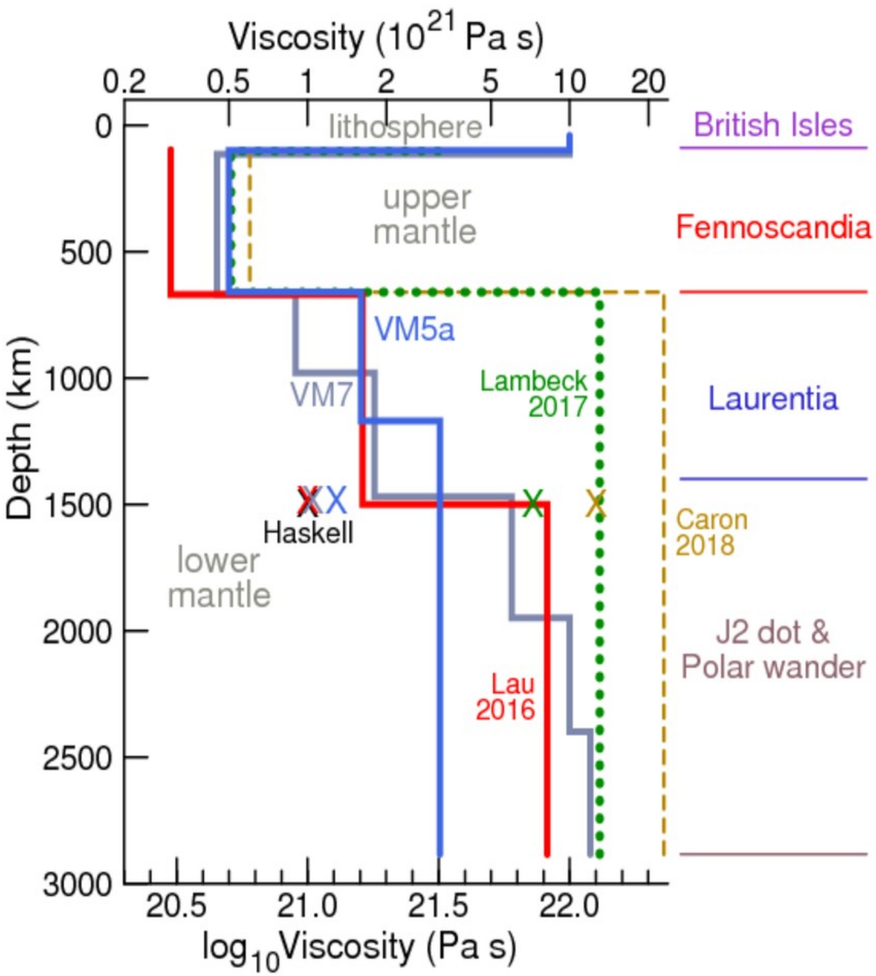

Argus et al (2021)

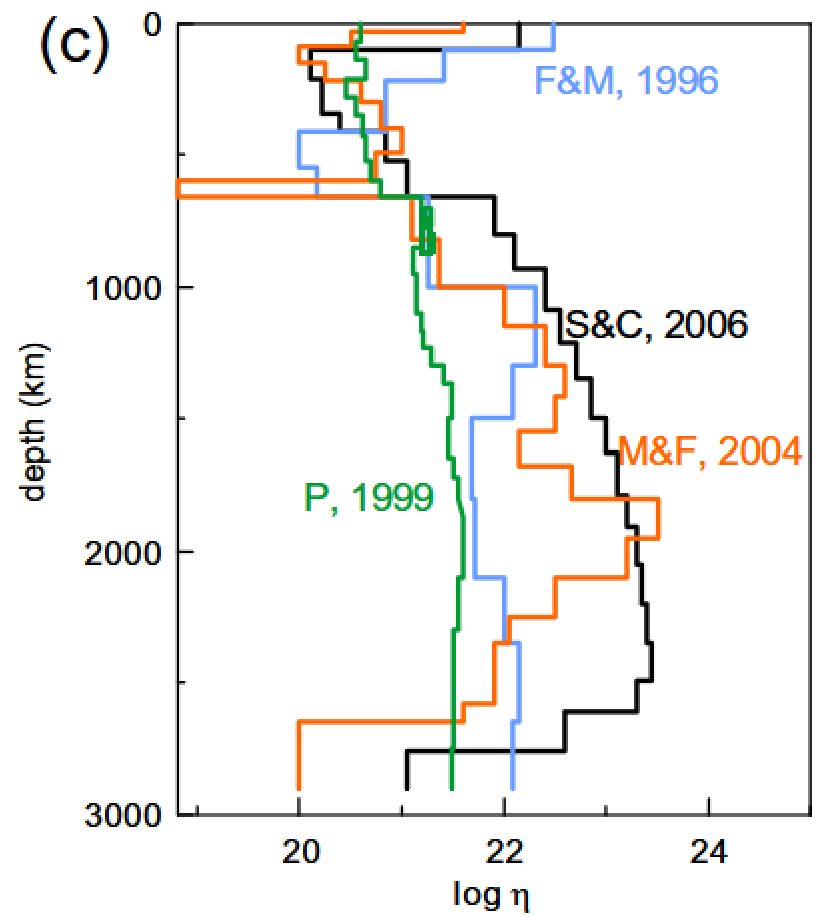

Cizkova et al (2012)

Impact on GPS solutions

Ivins et al. (2023)
Idealized disk load scenario
Comparable conditions
to modern ice mass loss

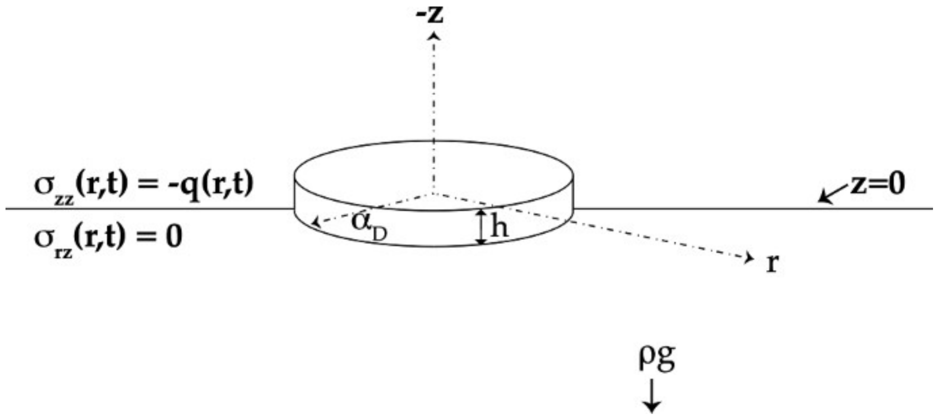

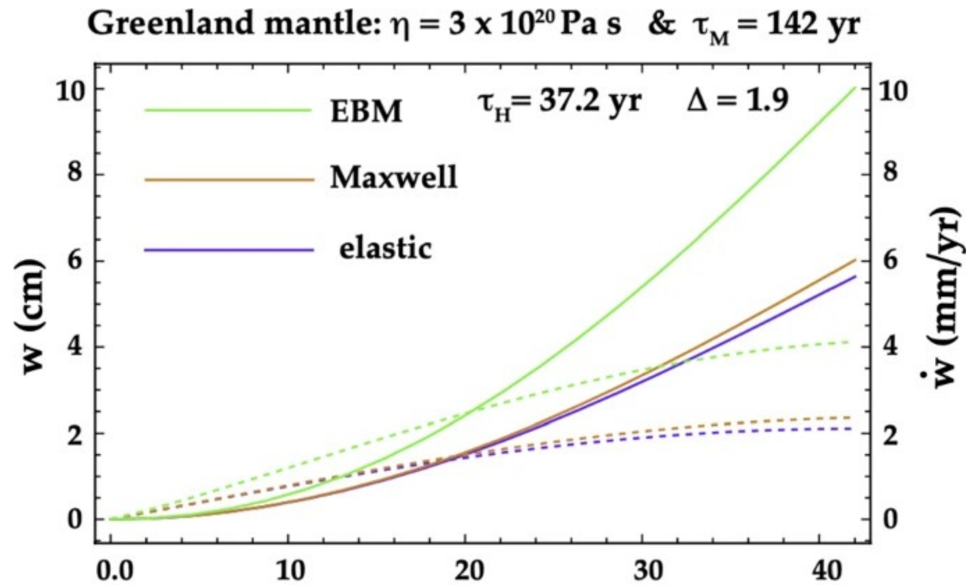

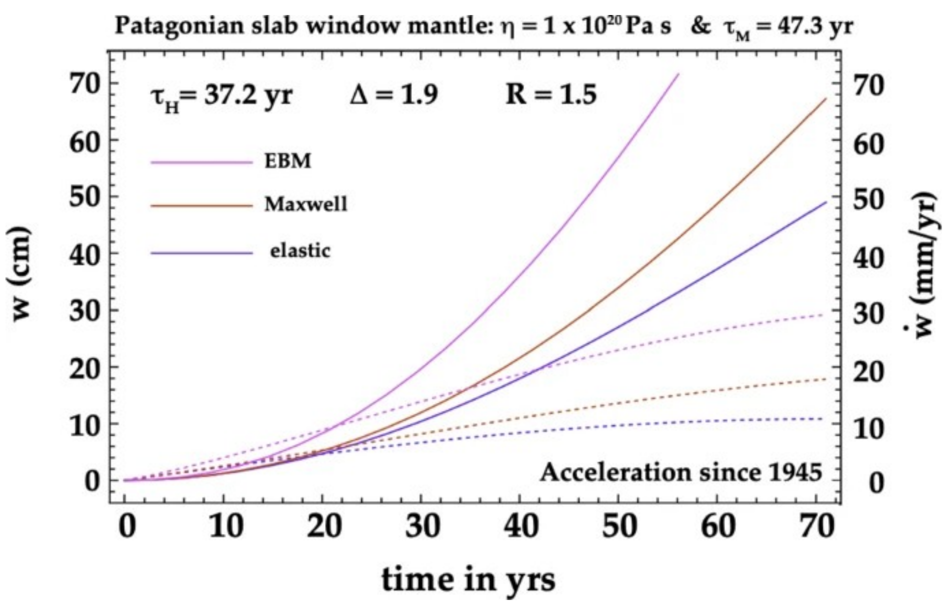

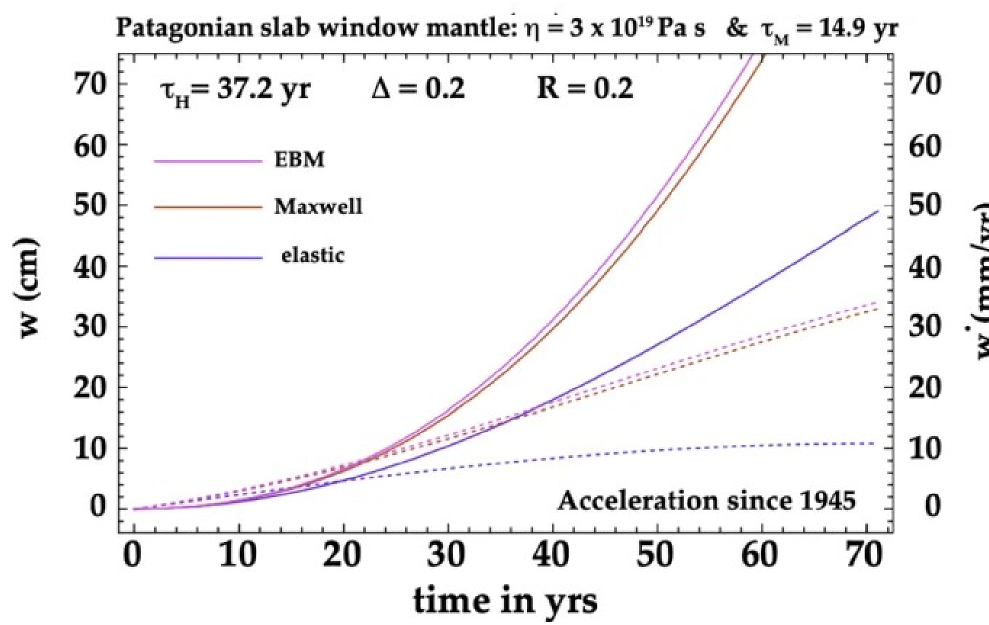

Impact on GRACE solutions

GRACE L3 processing assumes:
EWH = Gravity_potential / (1+ke)

What if the mantle is anelastic?

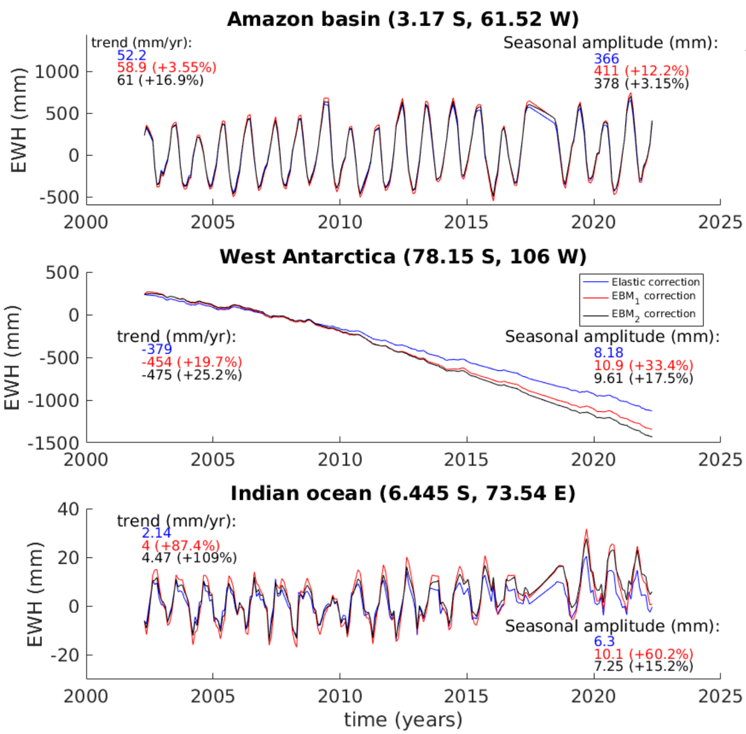

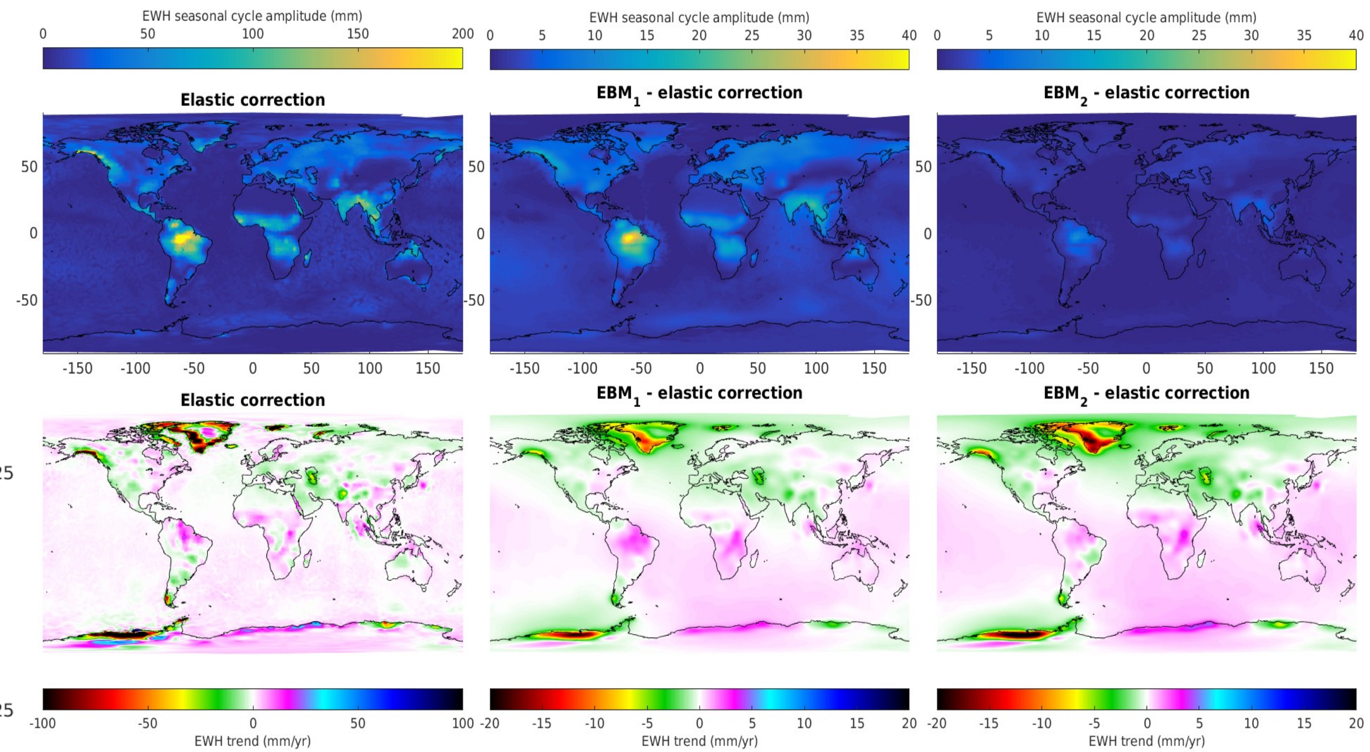

Top: seasonal cycle amplitude
Bottom: 20-year trend
Left: comparison of timeseries at 3 locations
Elastic model (blue)
EBM1 model (red): Δ=3, τH=1 month
EBM2 model (black): Δ=5, τH=5 years

Take-home messages

Evidence pointing to anelastic deformation on time scales ranging from hours to centuries (lab experiments, GNSS data, tides and rotation)

- Anelasticity on tidal time scales could partially be explained with Maxwell rheology, but not in a way that is consistent with geodynamic constraints

- Models using the Extended Burgers Material as the mantle rheology can reconcile estimates of the lower mantle viscosity from tidal data, GIA, and geodynamic constraints

- Transient relaxation time scales in EBM imply anelastic deformation on time scales relevant to GRACE and GNSS time series.